Updated Traffic Flow Dispersion Model Considering Effects of in-Vehicle Advisory Messages

Fengxiang Qiao*, Qing Li and Lei Yu

Innovative Transportation Research Institute, Texas Southern University, USA

Abstract

Traditional dispersion models; such as the travel time distribution based normal distribution model and geometric distribution model; are dedicated to traffic situations with conventional traffic signs and signals; which may not be able to depict the platoon dispersion phenomenon under a connected vehicle system with in-vehicle advisory messages. This research re-examines the traditional dispersion models with suitable adjustment considering impacts of in-vehicle messages. A correction factor was employed to update the travel time distribution model; while travel time distributions of leading vehicles with and without the in-vehicle messages were simulated in a driving simulator with forty-five subjects tested. Parameter calibrations for travel time dispersion of traffic flow in work zone and intersections with sun glares were conducted to illustrate the entire modeling and calibration procedure. With more practical simulations and field tests; the flow dispersion models can be further calibrated for more applications in traffic flow simulation and optimizations.

Introduction

Platoon dispersion of traffic flow is the deterioration in platoon integrity that changes the compactness of a platoon. There are several measures of platoon dispersion: 1) the change of gap between the same pairs of vehicles when travelling towards downstream; 2) the change of headway; 3) the change of traffic flow rate within portions of the platoon, which is the most commonly used measure of dispersion; or 4) the change of density in different portions of platoon. Dispersion is a function of the length of the platoon and the travel time from a given point to a downstream location (or sometimes a downstream stop-line) [1]. Obviously the longer the travel time is, the greater the dispersion would be as the longer the travel time would provide longer time (opportunity) for different drivers to deviate from the average travel time. For a given distance over a roadway segment (such as the distance between two traffic signals), there will be more dispersion of a slow speed traffic flow than that of a higher speed one. Typical flow dispersion models include the Normal Distribution Model by Pacey [2], the Geometric Model by Robertson [3], and the Neural Network System Identification Model by Qiao [4]. Some of these dispersion models have by now been incorporated into the famous traffic simulation and signal timing optimization programs such as TRANSYT (Traffic Network study tool) [5] and TRANSYT-7FTM [6], which are now widely used in the world for routine operations of traffic signals by serving millions of the public every day [4]. Since then, the calibration and implementation of traffic flow dispersion models seem to be a well-developed technology already [4,7,8].

However, in recent years, many innovative technologies in communication and computer engineering have advanced not only the revolution of vehicle designs, but also the operation of transportation systems. For example, the Connected Vehicle (CV) and Vehicle-to-Infrastructure (V2I) technologies could change drivers' behaviors, especially when vehicles are approaching the areas with traffic control guidance such as the work zones and intersections [9-11]. The space distributions of vehicle speeds, acceleration rates, the travel time, and thus the ways of dispersion could be totally changed [12-14]. Therefore, there is a need to re-examine the traditional traffic flow dispersion models, and make suitable adjustment accordingly.

With regard to this, this research is proposed to calibrate travel time based traffic flow dispersion models. A travel time factor was proposed to update the traffic flow dispersion model for the application of the V2I based Drivers' Smart Advisory System (DSAS). Driving simulator tests was conducted in simulated sequential intersections with sun glare disturbance as well as within a typical work zone area. The exact travel time and average driving speed of the leading vehicles that are instructed by the DSAS in the two study sites were recorded. Meanwhile, field observations were carried out at the intersection of NASA@HS 146, Webster Texas, and within the work zone area in Bellaire Blvd, in Houston Texas, to collect the driving speed variation of the vehicle platoon. A total of seventy-five subjects were recruited for the driving simulator tests, and the model parameters were carefully calibrated. The difference in the travel time distributions were visualized and compared.

Traffic Flow Dispersion Models

Normal distribution model

The diffusion theory proposed by Pacey [2] and investigated in detail by Grace and Potts [15] have shown to be adequate in describing the spreading of platoons in medium traffic flow without interference. According to Pacey's model, vehicles in a platoon travel in speeds v with mean $\bar{v}$ and standard deviation S. The arrival flow at the downstream section is the combination of the flows traveled from the upstream flow several time intervals ago, and the combination is governed by a kind of special normal distribution. The basic assumptions of the model are as follows: (l) vehicles in a platoon travelling at a certain speed follow a kind of transformed normal distribution; and (2) the speed of any individual car is unchanged as the car moves down the road. Mathematically, the downstream arrival flow is expressed as:

*Corresponding author: Fengxiang Qiao, PhD, Professor, Innovative Transportation Research Institute Texas Southern University, 3100 Cleburne Street, Houston, Texas - 77004 USA, Tel: 713-313-1915; Fax: 713-313-1856; E-mail: qiao_fg@tsu.edu

$$q_d(j) = \sum_{i=1}^{j} q_o(i) g(j-i) \qquad (1)$$

where, $q_0(i)$ is the upstream flow rate at time i; $q_d(j)$ is the downstream flow rate at time j; $g(T)$ is a special normal distribution function of travel time as is defined in equation (2).

$$g(T) = \frac{a}{T^2 S\sqrt{2\pi}} \exp\left[-\frac{(a/T - \bar{v})^2}{2S^2} \right] \qquad (2)$$

where,

T: Travel time between upstream and downstream points;

a: Length of the surveyed road segment;

$\bar{v}$: Average speed;

S: Standard deviation of the travel speed.

Geometric distribution model

An alternative method for predicting platoon dispersion has been given by Robertson [5], who used observed data to derive an empirical method of predicting the platoon behavior. The method was used for synchronization of traffic signals for minimum delay [16]. For each time interval it is assumed that the arrival flow at the downstream stop-line is found by the following recurrence equation:

$$qd(j) = Fq0^{(j-t)} + (1-F) \, qd^{(j-1)} - \qquad (3)$$

where

i: A counter of time interval at the upstream point;

j: A counter of time intervals at the downstream point;

t: 0.8 times the mean travel time;

$q_d(j)$: Predicted flow rate in interval j of the platoon at downstream point;

$q_0(i)$: Flow rate of the initial platoon in interval i at upstream point;

F: A smoothing factor defined as:

$$F = (1 + \alpha\beta T)^{-1} \qquad (4)$$

α: A dispersion factor, the best fit value is 0.5 based on a study by in West London;

β: The platoon arrival time coefficient, it is an empirical factor, generally 0.8;

T: As is defined before.

Some well-known traffic control systems, such as TRANSYT and SCOOT, use Robertson's model in Equation (3) to describe the dispersion of the platoon along a road segment. Seddon [17] reformatted equation (3) in a geometric distribution form.

$$q_d(j) = \sum_{i=1}^{j} q_o(i) F(1-F)^{j-t-i} \qquad (5)$$

By comparing Equation (5) and Equation (1), the Robertson's formula in Equation (3) is actually the same as that of Racey's except that the transferring normal function of travel time is now replaced by the geometric distribution [18]. Rumsey and Hartley [19] proved that the geometric distribution has a longer tail than the corresponding transformed normal distribution, which means the geometric distribution model predicts a wider platoon dispersion for any given mean travel time. Therefore, the distribution range of vehicles travelling according to the geometric distribution model is wider than that from the normal distribution model.

Intelligent dispersion model

Qiao et al. proposed an intelligent dispersion model based on a nonlinear mapping of a multi-input one output dynamic system, which is actually a one hidden layer feedforward sigmoid neural network model. The information set of the established neural network mode is as:

$$Z^N = [y(t-1),\ldots,y(t-n_y); u_1(t-k),\ldots, u_1(t-k-n_1), u_2(t-k),\ldots, u_2(t-k-n_2)] \qquad (6)$$

where, Z^N represents the information set of all available data, y represents the downstream flow with n_y observed data. u_1 and u_2 are the upstream flow and upstream speed, respectively. n_1 and n_2 are the numbers of the past upstream flow and the past upstream speed to be used as inputs to the neural network, respectively. k is the time delay. Normally, n_1, n_2 and n_y are called the orders of model. The predictor is:

$$\{\hat{y}(t/\hat{\theta})\} = \hat{y}(t/t-1,\hat{\theta}) \qquad (7)$$

where, $\hat{\theta}$ is the predicted value of parameter set. The neural network model under such regressors is called the Series-Parallel model [20] or the NNARX model [21].

In equation (7), $\hat{y}(t/\hat{\theta})$ is a "guess" of downstream traffic flow $y(t)$, providing that the information in Z^N and the particular parameter value $\hat{\theta}$ are given. The chronicle set $\hat{y}(t/\hat{\theta})$ is dispersed traffic flow at downstream.

Calibration of flow dispersion model from travel time distribution with V2I

In connected vehicle system, many studies demonstrate that the V2I messages would influence drivers' driving behavior, thereby altering vehicle speeds and accelerations [22-24]. Vehicles' travel time could also be changed accordingly. The travel time distribution $g(T)$ in equation (2) for normal distribution model and the smooth factor F in equation (3) for geometric distribution model would be varied. Assuming that the travel time with V2I is T_{V2I}, a time correction factor can be introduced and calculated as:

$$\gamma = \frac{TV_2I}{T} \qquad (8)$$

Thus, the calibrated travel time for normal distribution model is updated to:

$$g(T) = \frac{a}{(\gamma T)^2 S\sqrt{2\pi}} \exp\left[-\frac{(a/\gamma T - \bar{v})^2}{2S^2} \right] \qquad (9)$$

The calibrated smooth factor of geometric model is:

$$F = (1 + \alpha\beta\gamma T)^{-1} \qquad (10)$$

The newly introduced parameter γ can be calibrated from observed data. Since the V2I is still in its infant testing stage, the field test is not feasible. A driving simulator test could be one of possible options to calibrate the γ.

Testing travel time dispersion in simulator test

Driving simulator tests were chosen to measure the impacts of V2I message on the travel time of a leading vehicle. Meanwhile, speed standard deviation of a vehicle platoon was measured by field observations on an approach to an intersection and a work zone.

Apparatus

In this research, a fixed-base driving simulator (Drive Safety DS-600C) was employed, while the sun glare was artificially mimicked through an overhead projector as is illustrated in Figure 1.

Scenario design and test procedure for test bed at intersections with sun glare effects

Three scenarios were designed for the driving simulator test. Each scenario is coded with two letters in relation to two factors: (a) with sun glare (S) or without ($\overline{S}$); and (b) with the DSAS AWM (D) or without ($\overline{D}$). Figure 2 shows the layout of the scenario design with corresponding unique code. Each subject was requested to drive on a virtual track of approximately 3,000 meters in an industrial area. The speed limit on the track is 45mph (72 km/hr). As Figure 2 illustrated, there are three intersections. The distance between two sequential intersections is about 1,000 meters. Subjects experienced the situation with and without sun glare disturbance, and with the aid of DSAS warning message under sun glare effect at each intersection, respectively. The DSAS messages include "*Red Light is On*" and "*Green Light is On*", which last about 1 second. During the test, each subject was the only driver on the track. The only one visional disturbance is the sun glare in the simulation environment.

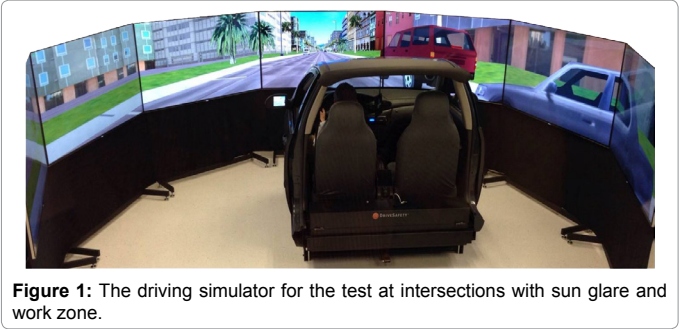The determination of locations to provide audio messages was

Figure 1: The driving simulator for the test at intersections with sun glare and work zone.
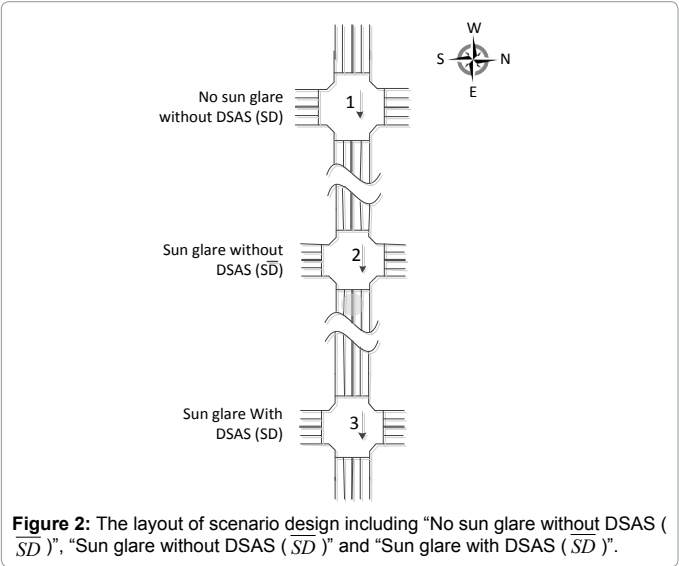

Figure 2: The layout of scenario design including "No sun glare without DSAS ($\overline{SD}$)", "Sun glare without DSAS ($S\overline{D}$)" and "Sun glare with DSAS (SD)".
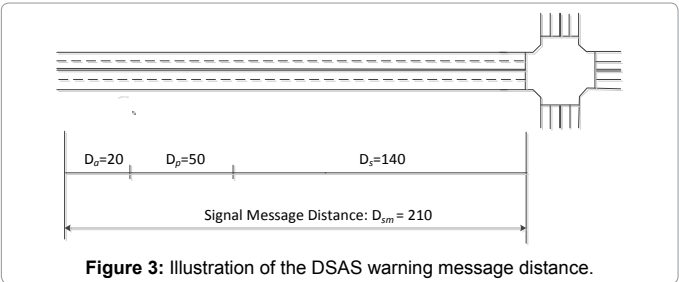

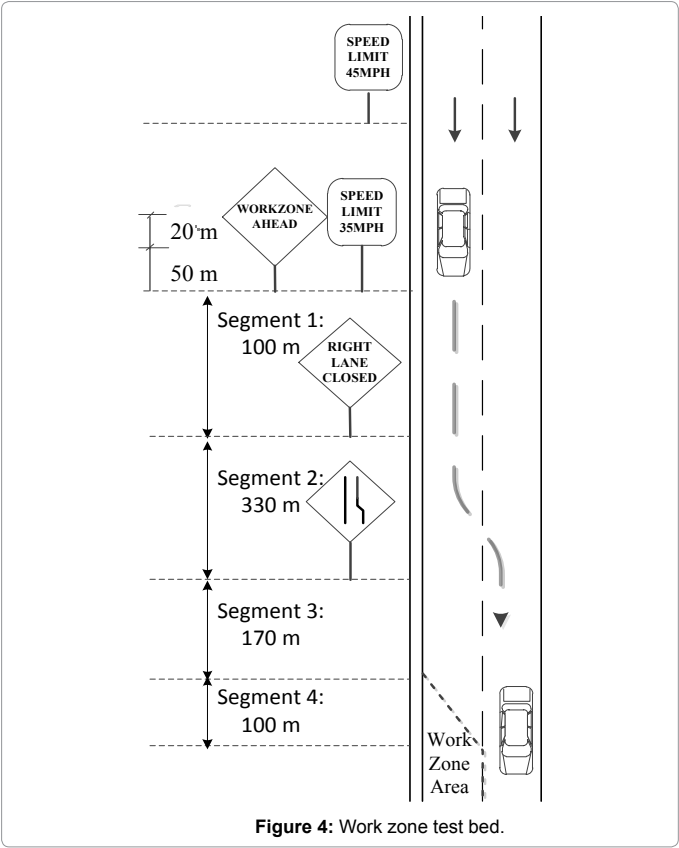**Figure 3:** Illustration of the DSAS warning message distance.

Figure 4: Work zone test bed.

Subjects	Gender		Age		Education background	
	Male	Female	<65	65 +	High school/Associate degree	Bachelor's degree or higher
Houston 2010 Census data	49.9%	50.1%	91.5%	8.5%	70.4%	27%
Adjusted Distribution for test	50%	50%	90%	10%	70%	30%
Subjects in test	15	15	27	3	21	9
Total	30		30		30	

Table 1: Demographic information of subjects for simulator tests.

based on human's perception-reaction time 2.5 second [24,25] (Travel distance in reaction time: D_a), the duration of the audio messages (Travel distance in audio playtime: D_p), and minimum sight distance (D_s) for the specific speed limit [26] (Figure 3). Therefore, for the speed limit of 72 km/hr, the total signal message distance of D_{sm} is: D_{sm} = D_a + D_p + D_s= 20m+50m+140m= 210m. Besides, the approach of each intersection was divided into three segments for speed deviation measurement.

Scenario design and test procedure for test bed in work zone

Figure 4 shows two scenarios designed for the work zone simulator test. Each work zone was divided into four segments for speed deviation measurement. Subjects drove through two work zones with and without the aid of DSAS messages, respectively. In the scenario with the DSAS messages, subjects received audio messages on the traffic control signs, such as "*Workzone Ahead*", "*Speed Limit Is 30 Mph*", and "*Right Lane Is Closed*". The distance to provide the audio messages is determined by the 2.5 seconds perception-reaction time [27,28] the duration of the audio messages (less than 1 second), and the speed limit.
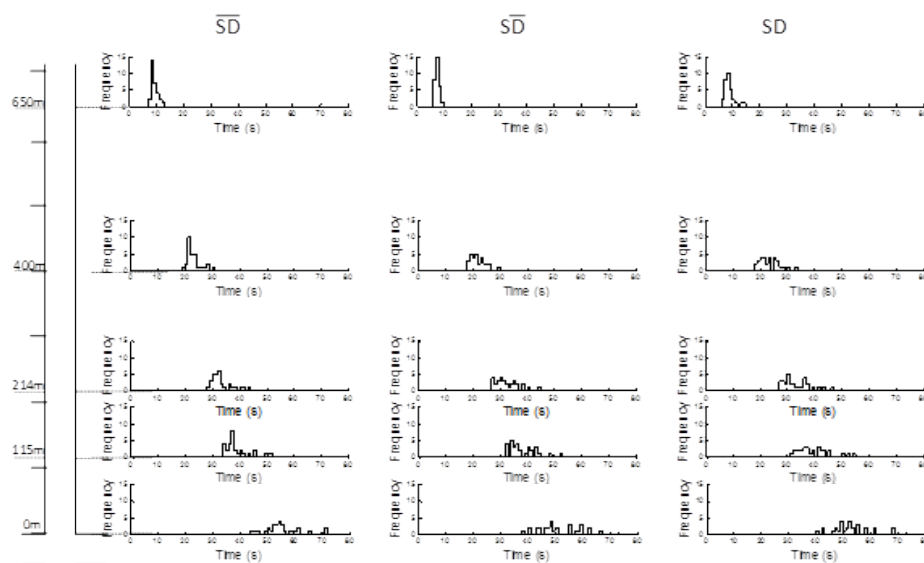
Figure 5: Distribution of the first vehicle in sun glare with and without DSAS messages.

Participants

Individual driving behaviors could be also subject to their demographic information, such as gender, age, and education level [29,30]. Therefore, subject recruitment was based on Houston demographics from 2010 census (Table 1). A total of 30 and 45 subjects were recruited for the driving simulator tests of intersection with sun glare and work zone, respectively. All subjects possess valid C class Texas driver license and have self-reported of normal or corrected-to-normal visions, and don't have any hearing problem.

Data collection and processing tools

During the driving simulator tests, the leading vehicle's real-time operation information was collected at a sampling rate of 60 Hz under the situation with and without the aid of the V2I DSAS messages. The collected operation information includes vehicle's geo-location, speed, and braking levels ranging from 0.0 to 1.0 (0.0 is the minimum with no brake and 1.0 the maximum with full brake). The collected data were processed to measure drivers' driving performance through a self-developed program in MATLAB, in terms of travel time and driving speed.

Field observations

Two field observations were conducted to obtain the speed deviations. The field observation I was carried at the intersection of NASA @ HS 146, Webster, TX. Video of vehicle movements on southbound approach were recorded from Houston Tran Star from 10:00 AM to 11:20 AM on August 20, 2014. A test vehicle started from 1,000 meters away the stop line of the downstream intersection and randomly joined in a vehicle platoon to approach the intersection. The test vehicle's speeds were measured at 210 meters, 190 meters, 140 meters, and zero meters (at the stop line), respectively, which were within the active area of the DSAS messages as shown in Figure 3. After passing the intersection, the test vehicle turned back to the start point for another round.

Field observation II was carried out within a road construction zone in Bellaire Blvd. in Houston, Texas, on August 21 in 2014. A test vehicle started from 1,480 meters (zero in Figure 4) away the work zone buffer area (the right lane is complete closed) to randomly join a vehicle platoon. The work zone buffer area was about 500-meter long. The test vehicle went through the work zone area and turned back to the start point for another round. The speeds were recorded at 700 meters, 600 meters, 270 meters, 100 meters, and zero meters to the work zone buffer area, respectively.

The sample size (N) of the joined vehicle platoons was determined using Equation (11) [31,32].

$$N = \frac{S^2 * Z^2}{E^2} \tag{11}$$

Where,

S: Standard deviation;

Z: z-score.

E: Acceptable errors.

Based on preliminary study, the S was approximately 7%. When the Z was set to 1.96, the sample size is able to meet a 95 percent conference level. In this study, 5% errors (E) was acceptable for driving speeds. It turns out that a minimum of 8 samples of vehicle platoons was required.

Testing Results

Intersections with sun glare disturbance

Distribution of the first vehicle from simulator tests and estimation of time factors: Figure 5 displays the travel time distribution of the first vehicle in each segment from simulator tests for three scenarios. As a whole, the travel time deviates widely with the increase in travel distance along the approach to an intersection. The deviations are obviously caused by the sun glare disturbance and the application of DSAS that is proposed to offset the sun glare interference.

The empirical factor β of 0.8 was adopted to calculate average travel time, namely 1/0.8 times of the first vehicle's travel time. As sun glare only affects the drivers approaching the intersection, only the travel

time during the segments in the first 400 m away to the intersection are compared in Table 2.

In Table 2 for segment 1, the average travel time with sun glare $S\overline{D}$ (13.97s) is shorter than that without sun glare $\overline{SD}$ (17.70s). When the DSAS is applied in the scenarios SD, the travel time is compensated back to some extent (15.14s). The time factor γ for the sun glare scenario is 0.79, while for the scenario of sun glare with DSAS message is 0.86.

Similar phenomenon can be found for segments 2 and 3, although the differences of travel time among different scenarios are normally less than 1s.

Field calibration of speed standard deviation at intersection approach: Table 3 lists the calculated mean speeds and standard deviation for the approach to the intersection from field observation I. Along with the approach to the intersection, the mean speeds decrease with higher standard deviations.

Comparison of travel time distributions with sun glare and DSAS messages: Figure 6 demonstrates the resulted travel time

Variables	Segment 1 (0-115 m)			Segment 2 (115-214 m)			Segment 3 (214-400 m)		
	$\overline{SD}$	$S\overline{D}$	SD	$\overline{SD}$	$S\overline{D}$	SD	$\overline{SD}$	$S\overline{D}$	SD
First vehicle travel time	14.16	11.18	12.11	6.04	5.60	6.04	4.66	4.81	4.66
Average travel time	17.70	13.97	15.14	7.55	7.00	7.55	5.82	6.01	5.82
Time Factor γ	1.00	0.79	0.86	1.00	0.93	1.00	1.00	1.03	1.00

Table 2: Average travel time and time factor for intersection approach with sun glare (Unit: s).

UP_Dispatch (240 m)	Segment 1 (0-100 m)	Segment 2 (100-193 m)	Segment 3 (193-293 m)
Mean Speed (m/s)	14.73	18.67	19.88
Standard Deviation (m/s)	1.95	1.78	1.67

Table 3: Speed standard deviation at intersection approach.
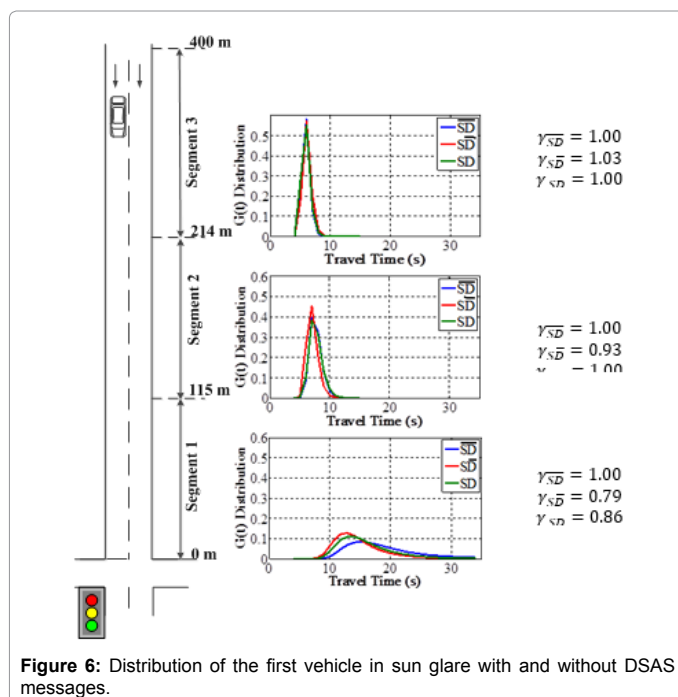

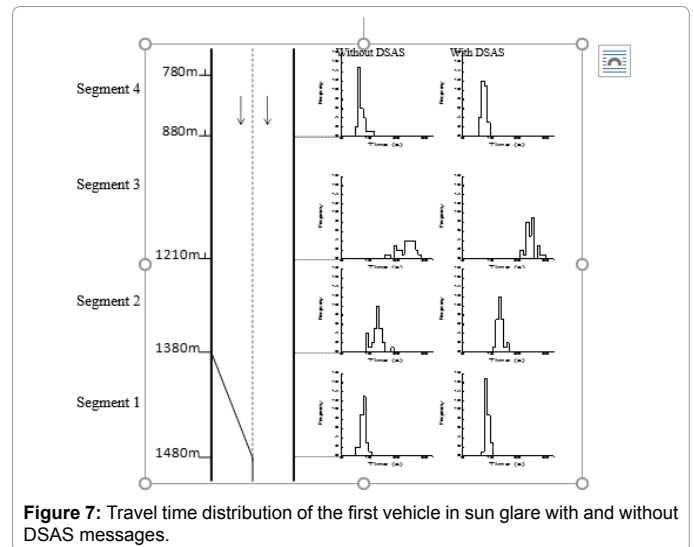**Figure 6:** Distribution of the first vehicle in sun glare with and without DSAS messages.

Figure 7: Travel time distribution of the first vehicle in sun glare with and without DSAS messages.

Variables	Segment 1 (1480-1380 m)		Segment 2 (1380-1210 m)		Segment 3 (1210-880 m)		Segment 4 (780-880 m)	
	$\overline{D}$	D	$\overline{D}$	S	$\overline{D}$	D	$\overline{D}$	D
First vehicle travel time	5.01	5.65	18.31	19.62	9.61	10.38	5.59	7.12
Average travel time	6.26	7.06	22.89	24.53	12.02	12.97	6.99	8.90
Time factor γ	1.13		1.07		1.08		1.27	

Table 4: Average travel time and time factor for work zone (Unit: s).

distribution based on normal distribution model in Equation (9) using the estimated average travel time and time factors γ in Table 2 and the observed speed deviation in Table 3.

In Figure 6 for segment 1, scenario $\overline{SD}$ represents the normal situation with no sun glare and no V2I DSAS message (the blue line). The time factor $\gamma_{S\overline{D}}$ is 1.00. In this case, Equation (8) is the same as Equation (2). For scenario $S\overline{D}$ and SD, however, $\gamma_{S\overline{D}} = 0.79$ and $\gamma_{SD} = 0.86$. The calibrated model in Equation (8) is used to calculate vehicle travel time (the red line and green line, respectively). The green line lies in between the red and blue lines, which means the V2I DSAS messages offset the difference caused by the sun glare disturbance at a certain level.

For segments 2 and 3, the time factors γ are all close to 1.00 and their speed standard deviations are close to each other as well. This implies that the impacts of both sun glare disturbance and V2I DSAS message are not so obvious, whether or not to use the calibrated dispersion models makes no significant difference.

Work zones

Distribution of the first vehicle from simulator tests and estimated time factors: Figure 7 shows the travel distribution of the first vehicle from the simulator tests. With the approaching to the work zone entrance, the distribution of travel time with DSAS message becomes narrower.

Table 4 lists the average travel time and time factors for both scenarios. Likewise, the average travel time was estimated by the first vehicle's travel time divided by the empirical factor β of 0.8. In all segments, the time factors γ are all greater than 1.00, meaning that the DSAS messages yield out longer travel time.

Field calibration of speed standard deviation: Table 5 lists the

Variables	Segment 4 (1480-1380 m)	Segment 3 (1380-1210 m)	Segment 2 (1210-880 m)	Segment 1 (780-880 m)
Mean Speed (m/s)	32.58	33.79	45.05	47.87
Std. Dev (m/s)	2.31	7.54	3.43	1.75

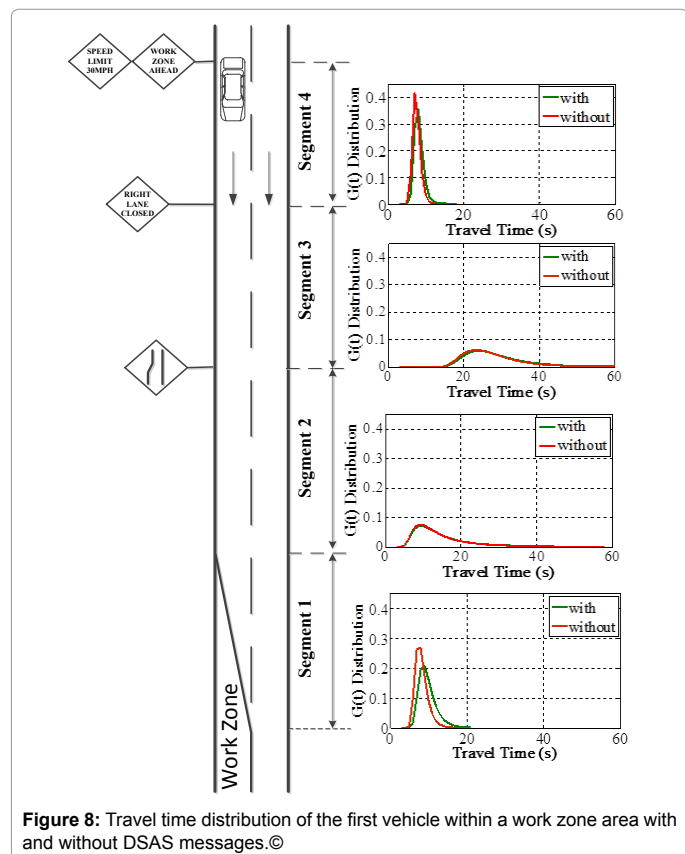**Table 5:** Speed standard deviation in work zone.

Figure 8: Travel time distribution of the first vehicle within a work zone area with and without DSAS messages.©

calculated mean speeds and standard deviation for the work zone entrance from field observation II, where the mean speeds decrease with the approaching to the work zone. Segment 2 is the transition area of the work zone, in where two lanes are merged into one lane. Significant deviation of vehicle speeds normally shows up in this area. Table 5 indicates that, the standard deviation (7.54 m/s) of speed in segment 3 is much higher than those for other segments.

Comparison of travel time distributions with and without DSAS messages: Figure 8 illustrates the travel time distribution from the calibrated distribution equation (8) using the average travel time and time factor γ in Table 4, and the speed standard deviations in Table 5. The distributions of travel time with (green lines) and without DSAS (red lines) differ the most for segment 1, while less for segments 2 and 3. The obvious difference in the segment 1 further demonstrates that the application of DSAS changes platoon's dispersion in the work zone. In such a situation, the updated calibrated travel time expressed by equation (8) is recommended for dispersion modeling.

Conclusion

To calibrate a travel time distribution in a platoon's dispersion, driving simulator tests and field observations were conducted in two critical traffic situations: an intersection and a work zone. The driving simulator tests were used to measure the travel time of the leading vehicle of a platoon, while field tests in one work zone and

one intersection were carried out to calibrate the relevant mean speed standard deviations. The travel time distribution model was calibrated by adding a time correction factor (γ). Results showed that the application of V2I DSAS affected the travel time of the first vehicle at varied levels. Besides, the time factors γ for the intersections and work zones are inconsistent in different situations, which means the travel time T in the traditional normal distribution models as well as in the geometric distribution models may not be able to provide a realistic result for vehicle platoon dispersion. The calibrated model is able to accurately express the dispersion evolution with the V2I DSAS message. With more practical simulations and V2I field tests, the flow dispersion models can be further calibrated for more applications in traffic flow simulation and optimizations.

Acknowledgement

References

1. Messer CJ, Fambro DB, Andersen DA (1975) A studies of the effects of design and operational performance of signal systems - Final Report.

2. Pacey GM (1956) The progress of a bunch of vehicles released from a traffic signal. London: Road Research Laboratory.

3. Robertson A (1967). The nature of quantitative genetic variation. In: Brink RA and Styles ED (eds), Heritage from Mendel. University of Wisconsin Press, Madison, WI p: 265-280.

4. Qiao F (2010) Intelligent data dependent modeling of traffic flow: solving problems in traffic flow classification, simulation, and control. ISBN-10: 3838329066, ISBN-13: 978- 3838329062, LAP Lambert Academic Publishing, UK.

5. Robertson DI (1969) TRANSYT: A traffic network study tool.

6. Wallace CE, Courage KG, Chang ECP (1991). Methodology for Optimizing Signal Timing -- The M|O|S|T Reference Manual, Volume 1 of a series prepared for FHWA by Courage and Wallace, Gainesville, FL.

7. Rouphail NM (1983) Analysis of transyt platoon-dispersion algorithm (No. HS-036 189).

8. Stankiewicz B (1995) LCAO study of the density of states of Ge/RbF. Vacuum 46(5): 541-544.

9. Qiao F, Jia J, Yu L (2013) A short range vehicle to infrastructure system at work zones and intersections. In: 20th ITS World Congress, Japan.

10. Qiao F, Jia J, Yu L, Li Q, Zhai D (2014) Drivers' Smart Assistance System Based on Radio Frequency Identification: Enhanced Safety and Reduced Emissions in Work Zones. Transportation Research Record: Journal of the Transportation Research Board. 1(2458): 37-46.

11. Li Q, Qiao F, Wang X, Yu L (2016) Drivers Smart Advisory System Improves Driving Performance at STOP Sign Intersections. Journal of Traffic and Transportation Engineering (English Edition).

12. Qiao F, Rahman R, Li Q, Yu L (2016) Identifying Smartphone Based Intelligent Messages for Worker's crossing in Work Zones. Journal of Transportation Technologies. 166(02): 76.

13. Li Q, Qiao F, Yu L (2016) Calibration of car-following models considering the impacts of warning messages from tablet/smartphone application. Journal of Transportation Technologies. 166(2): 61.

14. Li Q, Qiao F, Yu L (2016) Implications of Advanced Warning Messages on Eliminating Sun Glare Disturbances at Signalized Intersections. Journal of Traffic and Transportation Engineering (English Edition). 3(4).

15. Grace MJ, Potts RB (1964). A theory of the diffusion of traffic platoons. Opl Res 12: 255-275.

16. Hillier JA, Rothery R (1967) The synchronization of traffic signals for minimum delays. Transportation Science 1(2): 81-94.

17. Seddon PA (1972) Another look at platoon dispersion: III. The recurrence relationship. Traffic Engineering and Control. 13(10): 442-444.

18. Qiao F, Yang H, Lam WH (2001) Intelligent simulation and prediction of traffic flow dispersion. Transportation Research Part B: Methodological. 30-35(9): 843-863.

19. Rumsey AF, Hartley MG (1972) Simulation of a pair of intersections. Traffic Engineering and Control.13(11/12): 522-525.

20. Narendra KS, Parthasarathy K (1990) Identification and control of dynamical systems using neural networks. IEEE Transactions on neural networks. 1(1): 4-27.

21. Sjoberg T, Zhang Q, Ljung L, Benveniste A, Delyon B, et al. (1995) Nonlinear black-box modeling in system identification: a unified overview. Autom. 31(12): 1691-1724.

22. Li Q, Qiao F (2014) How drivers' smart advisory system improves driving performance? A simulator imitation of wireless warning on traffic signal under sun glare. Lambert Academic Publishing. ISBN-13: 978-3-659-57193-0.

23. Li Q, Qiao F, Wang X, Yu L (2015) Driving performance test of stop signs with drivers smart advisory system. In: Proceedings of the 28th Annual Conference of the International Chinese Transportation Professionals Association (ICTPA). p: 14-16.

24. Rahman R, Qiao F, Li Q, Yu L, Kuo PH (2015) Smart phone based forward collision warning messages in work zones to enhance safety and reduce emissions. In: Transportation Research Board 94th Annual Meeting 2015 (No. 15-0648).

25. Chang MS, Messer CJ, Santiago AJ (1985) Timing traffic signal change intervals based on driver behavior.

26. Manual on Uniform Traffic Control Devices (MUTCD) for Streets and Highways (2009) 2009 MUTCD with Revisions 1 and 2, May 2012, Section 4D.12.

27. Li Q, Qiao F, Yu L (2015) Socio-demographic impacts on lane-changing response time and distance in work zone with drivers' smart advisory system. Journal of Traffic and Transportation Engineering (English edition). 2(5): 313-326.

28. Li Q, Qiao F, Yu L (2015) Fuzzy lane-changing models with socio-demographics and Vehicle-to-Infrastructure system based on a simulator test. The Journal of Ergonomics 5: 100-144.

29. Qiao F, Rahman R, Li Q, Yu L (2016) Identifying demographical effects on speed patterns in work zones using smartphone based audio warning message system. Journal of Ergonomics 6(2).

30. Robertson DI (1969) TRANSYT: A traffic network study tool. RRL Report LR 253, Road Research Laboratory, UK.

31. Roess RP, Prassas, ES, McShane WR (2009) Traffic Engineering, (4thedn). Pearson, Prentice Hall, Upper Saddle River, New Jersey.

32. Robertson HP, Thomas WN (1968) Relativity and Cosmology. Brockport Bookshelf. Book-253.